THE JOURNAL OF BIOLOGICAL CHEMISTRY VOL. 286, NO. 23, pp. 20398–20406, June 10, 2011

Arabidopsis Monothiol Glutaredoxin, AtGRXS17, Is Critical for Temperature-dependent Postembryonic Growth and Development via Modulating Auxin Response*[S]

Received for publication, November 8, 2010, and in revised form, March 30, 2011 Published, JBC Papers in Press, April 22, 2011, DOI 10.1074/jbc.M110.201707

Ning-Hui Cheng[‡1], Jian-Zhong Liu[§], Xing Liu[¶], Qingyu Wu[‖], Sean M. Thompson[**], Julie Lin[‡], Joyce Chang[‡], Steven A. Whitham[§], Sunghun Park[‖], Jerry D. Cohen[¶], and Kendal D. Hirschi[‡]**

*From the [‡]United States Department of Agriculture/Agricultural Research Service, Children's Nutrition Research Center, Baylor College of Medicine, Houston, Texas 77030, the [§]Department of Plant Pathology, Iowa State University, Ames, Iowa 50011, the [¶]Department of Horticultural Science and Microbial and Plant Genomics Institute, University of Minnesota, St. Paul, Minnesota 55108, the [‖]Department of Horticulture, Forestry and Recreation Resources, Kansas State University, Manhattan, Kansas 66506, and the **Vegetable and Fruit Improvement Center, Texas A&M University, College Station, Texas 77845*

Global environmental temperature changes threaten innumerable plant species. Although various signaling networks regulate plant responses to temperature fluctuations, the mechanisms unifying these diverse processes are largely unknown. Here, we demonstrate that an *Arabidopsis* monothiol glutaredoxin, AtGRXS17 (At4g04950), plays a critical role in redox homeostasis and hormone perception to mediate temperature-dependent postembryonic growth. *AtGRXS17* expression was induced by elevated temperatures. Lines altered in *AtGRXS17* expression were hypersensitive to elevated temperatures and phenocopied mutants altered in the perception of the phytohormone auxin. We show that auxin sensitivity and polar auxin transport were perturbed in these mutants, whereas auxin biosynthesis was not altered. In addition, *atgrxs17* plants displayed phenotypes consistent with defects in proliferation and/or cell cycle control while accumulating higher levels of reactive oxygen species and cellular membrane damage under high temperature. Together, our findings provide a nexus between reactive oxygen species homeostasis, auxin signaling, and temperature responses.

Postembryonic growth and development in plants is drastically affected by many external factors, including light and temperature (1, 2). Plants have developed elaborate measures to sense environmental changes and adapt their growth and development accordingly (3). In particular, temperature perception and heat stress responses involve many genes and signaling pathways (4–7). For example, both hormone and reactive oxygen species (ROS)[2] are key mediators in regulating plant responses to temperature variations. However, the identity of early molecular components in this signal transduction pathway has remained enigmatic (5, 6).

Auxin is a phytohormone that is involved in most of, if not all, aspects of plant growth and development (8–11). It has been postulated that auxin plays an essential role in stress-induced growth and morphogenic responses (2). Previous studies also indicated that elevated temperature can regulate hormone biosynthesis and subsequently alter cell growth, morphology, and flowering time (12–15). The complexity of auxin signaling often obscures efforts to integrate this seemingly ubiquitous signal with specific signaling pathways.

ROS can be formed as by-products in all oxygenic organisms during aerobic metabolism (16). Plants also actively generate ROS as signals through activation of various oxidases and peroxidases in different cellular compartments in response to internal developmental cues and/or external environmental changes (17–19). There is growing evidence that there is cross-talk between the ROS-mediated redox signal (redox homeostasis) and hormonal action and response during plant development and adaptation to stress conditions, as occurs during seed germination, root hair development, stomata closure, and root gravitropic responses (20–24). Recent work suggests that redox status directly affects auxin signaling to alter growth (25). Triple mutants of *Arabidopsis* altered in key components of redox signaling display phenotypes consistent with perturbed auxin transport and metabolism (25). However, in that study (25), the contribution of specific ROS gene products to auxin signaling could not be determined, and no efforts were made to establish cross-talk between these pathways and the temperature response.

The thioredoxin and Grx enzyme systems help to control cellular redox potential (26). Grxs are ubiquitous small heat-stable disulfide oxidoreductases which are conserved in both prokaryotes and eukaryotes (27). Although plant genomes con-

* This work was supported by United States National Science Foundation Grants MCB-0725149, OIS-PGRP-0606666, OIS-PGRP-0923960, and PGRP-0820642 and the United States Department of Agriculture, National Research Initiative 2005-35318-16197 (to J. D. C. and S. A. W.) and United States Department of Agriculture/Agricultural Research Service under Cooperation Agreement 6250-51000-055 (to N.-H. C.). This work was also supported by National Science Foundation Grant NSF 90344350) and Designing Foods for Health Grant CSREES 2005-34404-16401) (to K. D. H.).

[S] The online version of this article (available at http://www.jbc.org) contains supplemental Figs. 1–3.

[1] To whom correspondence should be addressed: United States Department of Agriculture/Agricultural Research Service, Children's Nutrition Research Center, Baylor College of Medicine, Houston, TX 77030. Tel.: 713-798-9326; Fax: 713-798-7101; E-mail: ncheng@bcm.tmc.edu.

[2] The abbreviations used are: ROS, reactive oxygen species; Grx, glutaredoxin; ANOVA, analysis of variance; NPA, *N*-1-naphthylphthalamic acid; IAN, indoleacetonitrile; SPE, solid phase extraction; GC-SIM-MS, gas chromatography-selected ion monitoring-mass spectrometry; GUS, β-glucuronidase; IAA, indole-3-acetic acid.

tain many Grxs (28, 29), only a few have been characterized (30). A recent report indicates that an *Arabidopsis* Grx interacts with a transcription factor to alter defense responses (31). We previously demonstrated that both AtGRXcp (also termed *AtGRXS14*) and *AtGRX4* (also termed *AtGRXS15*) play a pivotal role in protecting the cell against oxidative stress (32, 33). However, the function of plant Grxs in diverse stress responses remains to be explored.

In the present study, we have characterized an *Arabidopsis* monothiol Grx, AtGRXS17, and describe altered expression of AtGRXS17 at an elevated temperature. Characterization of mutant phenotypes indicated alterations in ROS signaling, auxin responses, and thermo-sensitivity. These findings offer a clue to the elaborate regulatory interplay between ROS and auxin signaling in response to a heat stress.

EXPERIMENTAL PROCEDURES

Isolation of AtGRXS17-null Alleles and Creation of AtGRXS17 RNAi Lines—To isolate *atgrxs17* alleles, a T-DNA insertional mutant line, was obtained from the SALK T-DNA collection (SALK_021301) (34). Homozygous plants from the T3 generation were obtained by PCR screening using an *AtGRXS17* reverse primer (5′-TAG CTC GGA TAG AGT TGC TTT-3′) and a T-DNA left border primer (5′-GCG TGG ACC GCT TGC TGC A-3′) for *atgrxs17* allele; an *AtGRXS17* forward primer: 5′-ATG AGC GGT ACG GTG AAG GAT-3′ and the *AtGRXS17* reverse primer were used for identifying the wild type. The location of the T-DNA insertion was determined by sequencing the PCR product. The *atgrxs17* allele was backcrossed to wild type to remove any potential unlinked mutations. To generate *AtGRXS17* RNAi lines, the *AtGRXS17* cDNA was cloned into the binary vector pCHF3 with opposite orientation (supplemental Fig. 1*B*; 35). The antisense construct was transformed into *Agrobacterium* GV3101 strain, and then the positive strains were used to transform *Arabidopsis* Col-0 plants using the floral-dip method (36). The transgenic progeny were selected by kanamycin resistance. *AtGRXS17* expression levels in both *atgrxs17* knock-out and *AtGRXS17* RNAi plants were examined using semi-quantitative RT-PCR.

Plant Growth Conditions—Wild type (ecotype Columbia, Col-0), *atgrxs17* KO, *AtGRXS17* RNAi seeds were surface-sterilized, germinated, and grown on one-half strength Murashige and Skoog (MS) medium solidified with 0.8% agar or MS supplemented with various concentrations of phytohormones, as described previously (37). For quantitative RT-PCR analysis of *AtGRXS17* tissue distribution, total RNA was extracted from 5-week-old *Arabidopsis* wild type leaves, roots, stems, and flowers. To examine AtGRXS17 expression under heat stress, seeds were germinated and grown at 22 °C for 10 days, and seedlings were moved to 28 °C for 3, 6, 24, and 48 h, respectively, whereas control seedlings were kept at 22 °C. Root tips (~3 mm from the tip) were collected and pooled from each treatment. Total RNA was extracted and quantitative RT-PCR was performed with 18 S rRNA used for normalizing the data (38). For the root gravitropism assay, surface-sterilized wild type, *atgrxs17* KO, and *AtGRXS17* RNAi seeds were germinated and grown on one-half strength MS medium. All plates were sealed with 3M surgical tape and cultured vertically at 22 or at 28 °C with illumination by cool white fluorescent light under a 16 h light/8 h dark cycle for 5 days. Digital images were taken before the seedlings were gravistimulated for 24 h. (The plates were turned 90° clockwise.) Digital images were again taken to determine the angle of root growth deviation following gravistimulation. The angles of the root deviation were scored in 30° segments as described previously (39). For each line, three independent replicates were assayed using 140–144 seedlings. Data were analyzed using three-way ANOVA.

AtGRXS17-GUS Transgenic Plants, GUS Reporter Lines, and Histochemical Analysis—A 2.0-kb DNA sequence upstream of the ATG of the *AtGRXS17* ORF was amplified from genomic DNA using the *AtGRXS17* promoter forward and reverse primers (forward primer, 5′-CCC AAG CTT ATT GCT TGT TGT AAC TAA TGT-3′; reverse primer, 5′-GGC TCT AGA CTT CGA AGA GGG AGA AGG ATC-3′). The PCR fragment was cloned into pBI121 to replace the 35 S promoter, resulting in the plasmid pAtGRXS17-GUS. *Agrobacterium*-mediated transformation of *Arabidopsis* plants was performed as described previously (32). A DR5-GUS reporter line and a *Cyclin B1;1*-GUS reporter lines (a gift from Dr. Robert Sablowski) (40) were intergressed into *atgrxs17* KO and *AtGRXS17* RNAi lines. Histochemical analysis was performed following the previously published protocol (32). Thirty seedlings from each genotype and treatment were scored for GUS activity. Expression levels were considered strong when meristematic tissues and vascular bundle tissues displayed GUS activity. Weak expression was scored when few or no cells in the root meristematic region stained for GUS activity. Data were analyzed using two-way ANOVA.

Ion Leakage Measurement and Anthocaynin Determination—Four-week-old wild type and *atgrxs17* KO plants were subjected to heat stress at 38 °C in a growth chamber for 10, 20, and 40 h, respectively. During heat stress, plants were maintained at a relatively high humidity (~85%) in the growth chamber to minimize water loss from the plants. For electrolyte leakage, leaf samples were incubated in 15 ml of distilled water for 10 h to measure the initial electrolyte leakage using a conductance meter (Model 32, YSI, Inc., Yellow Springs, OH). The samples were subjected to 80 °C for 2 h to release the total electrolytes and then held at room temperature for 10 h. The final conductivity of the leachate was measured to determine the percent electrolyte leakage from the leaf samples. For anthocyanin quantitation, 0.1 g of fresh weight of wild type and *atgrxs17* KO seedlings, grown on one-half strength MS medium for 2 weeks at either 22 or 28 °C, homogenized in 1.6 ml of extraction buffer (0.6 ml of methanol-1% HCl, 0.4 ml of H_2O, and 0.6 ml of chloroform), and mixed well before spinning for 2 min at 16,000 × *g*. One ml of supernatant was used to measure the absorbance at 535 nm. The amount of anthocyanin is expressed as cyanidin 3-glucoside equivalents (mg·0.1 g of fresh weight^{-1}) (41).

Quantification of Free and Conjugated IAA—Ten-day-old wild type, *atgrxs17* KO, and *AtGRXS17* RNAi seedlings were harvested after growth at 22 or 28 °C. For each seedling type, 150–200 mg of frozen tissue was homogenized using a Mixer Mill (MM 300; Qiagen, Valencia, CA), with a 3-mm tungsten carbide bead in 300 μl of homogenization buffer (35% of 0.2 M imidazole, 65% isopropanol, pH 7) containing 20 ng of

[$^{13}C_6$]IAA and 200 ng of [^{13}C]indoleacetonitrile (IAN) as internal standards (42). After 1 h on ice, 150 μl of the homogenate was purified through two sequential solid phase extraction (SPE) columns, anion exchange and plastic affinity, using a Gilson SPE 215 system, methylated, dried, and redissolved in ethyl acetate exactly as described previously (43). The flow-through from the amino anion exchange SPE column was collected for IAN analysis. The samples were then analyzed using gas chromatography-selected ion monitoring-mass spectrometry (GC-SIM-MS) on an Agilent 6890/5973 system. The level of free IAA was quantified by isotope dilution analysis based on the [$^{13}C_6$]IAA internal standard (43). For IAN analysis, the flow-through collected from the amino SPE column was passed through a C18 SPE column (100 mg; Varian) and then washed with 3 × 0.6 ml water, eluted with 3 × 0.3 ml acetonitrile, evaporated to complete dryness, and derivatized with 50 μl of bis(trimethylsily)trifluoroacetamide plus 1% trimethylchlorosilane at 45 °C for 45 min. The samples were analyzed using GC-SIM-MS, and the correction factor for nonenzymatic conversion of IAN to IAA was determined (42). For the rest of the homogenate, 100 μl was hydrolyzed in 1 N NaOH (1 h, room temperature) for measurement of free plus ester-linked IAA, and 50 μl was hydrolyzed in 7 N NaOH (3 h, 100 °C under nitrogen gas) for measurement of total IAA. After hydrolysis, the pH of the homogenate was adjusted to 2.7 and desalted by passing through a C18 SPE column (100 mg; Varian), washed with 3 × 0.6 ml water, eluted with 3 × 0.3 ml methanol, evaporated to dryness, and redissolved in 150 μl of homogenization buffer. The purification of IAA released from the conjugates was subsequently the same as used for the purification of free IAA. The samples were analyzed using GC-SIM-MS, and the levels of free plus ester-linked IAA and total IAA were quantified with correction for IAN hydrolysis (42).

Polar Auxin Transport in Arabidopsis Hypocotyls—The hypocotyl basipetal IAA transport assay was modified from that described previously (44, 45). Wild type, *atgrxs17* KO, and *AtGRXS17* RNAi line seeds were surface-sterilized and plated on one-half strength MS medium. After 3 days in the dark at 4 °C and 12 h under cool white fluorescent lights (photosynthetically active radiation = 80 μmol m^{-2} s^{-1}), the seeds were grown at either 22 or 28 °C continuously in darkness for 4 days and then exposed to continuous cool white fluorescent lights (photosynthetically active radiation = 80 μmol m^{-2} s^{-1}) for an additional 2 days. Six mm of the hypocotyl section directly below the shoot apex was placed on an agar plate after excision, and an auxin donor agar block of 1.5% agar containing 0.2 M MES (pH 6.5) and 10^{-7} M [^{3}H]IAA was placed in contact with the apical end of the tissue section, whereas a receiver agar block containing 0.2 M MES (pH 6.5) was placed in contact with the basal end. Receiver blocks containing 0.2 M MES (pH 6.5) and 10 μM *N*-1-naphthylphthalamic acid (NPA) were used as the NPA control, and the orientation of the tissue section was inverted in the acropetal control. Two strips of polyethylene film (Saran^{TM} Original, S.C. Johnson & Sons, Inc.) were placed between the agar blocks and the support agar on the plates to avoid diffusion of [^{3}H]IAA and thus avoid an undesirable increase in background counts. The agar plates were placed vertically with donor blocks down in a chamber with maximal humidity for 4 h, and each of the hypocotyl sections was then divided into apical and basal halves. The receiver block and each half-section of the hypocotyl were incubated individually in scintillation mixture overnight, and the radioactivity was determined using a liquid scintillation counter (LS 6500, Beckman Coulter). Data were analyzed using one- and two-way ANOVA.

ROS Production and Measurement—For hydrogen peroxide staining, wild type and *atgrxs17* KO seedlings were grown at 22 and 28 °C for 10 days, respectively, and vacuum-infiltrated with 1 mg/ml 3,3′-diaminobenzidine in 50 mM Tris acetate buffer, pH 5.0. Samples were incubated for 4 h at room temperature in the dark before transferring to 96% ethanol. Thirty seedlings from each genotype and treatment were scored based on the brown-colored deposition in root tips, vascular bundles, and the root-hypocotyl junction. Data were analyzed using a chi-square test.

RESULTS

AtGRXS17 Expression in Response to High Temperature—The expression of *AtGRXS17* under normal growth conditions was detected in all tissues using quantitative RT-PCR (Fig. 1*A*). *AtGRXS17* expression appeared lower in mature leaves and higher in roots and flowers (Fig. 1*A*). In line with this observation, histochemical analysis of *AtGRXS17*-GUS transgenic plants showed expression in young cotyledons (*arrowhead*), growing leaves (*arrow*), roots, anthers, and developing embryos (Fig. 1, *B–E*). Interestingly, *AtGRXS17* expression was induced in young seedlings exposed to elevated temperature for 24 h (Fig. 1*F*). These results are in agreement with public microarray data sets (Genevestigator) and suggest that *AtGRXS17* is a temperature-responsive gene.

atgrxs17 KO and AtGRXS17 RNAi Lines Display Growth Defects—To understand the function of AtGRXS17 *in planta*, we identified a T-DNA insertion line. In the *atgrxs17-1* allele, the T-DNA insertion was located in the second exon (supplemental Fig. 1*A*). *AtGRXS17* expression was not detected in *atgrxs17-1* using semi-quantitative RT-PCR (supplemental Fig. 1*A*). We termed *atgrxs17-1* as *atgrxs17* KO. We then generated >60 independent RNAi lines using an *AtGRXS17* antisense RNA construct (supplemental Fig. 1*B*). *AtGRXS17* expression levels were variable among individual RNAi lines (supplemental Fig. 1*B*). Three RNAi lines that showed lower levels of *AtGRXS17* expression were selected for further phenotypic analyses. Both *atgrxs17* KO and *AtGXRS17* RNAi seeds germinated in a manner indistinguishable from wild type on one-half strength MS medium under normal growth conditions (22 °C); however, KO and RNAi seedlings had shorter primary roots (~25%) than wild type controls (Fig. 2, *A* and *C*). In addition, KO and RNAi seedlings had fewer growing leaves in comparison with wild type controls (supplemental Fig. 1, *C* and *E*). In soil at 22 °C, the mutant plants grew shorter inflorescence stems but flowered and produced seeds (Fig. 2, *F* and *G* and supplemental Fig. 1, *G* and *H*). These results suggest that AtGRXS17 plays a critical role in postembryonic growth in plants.

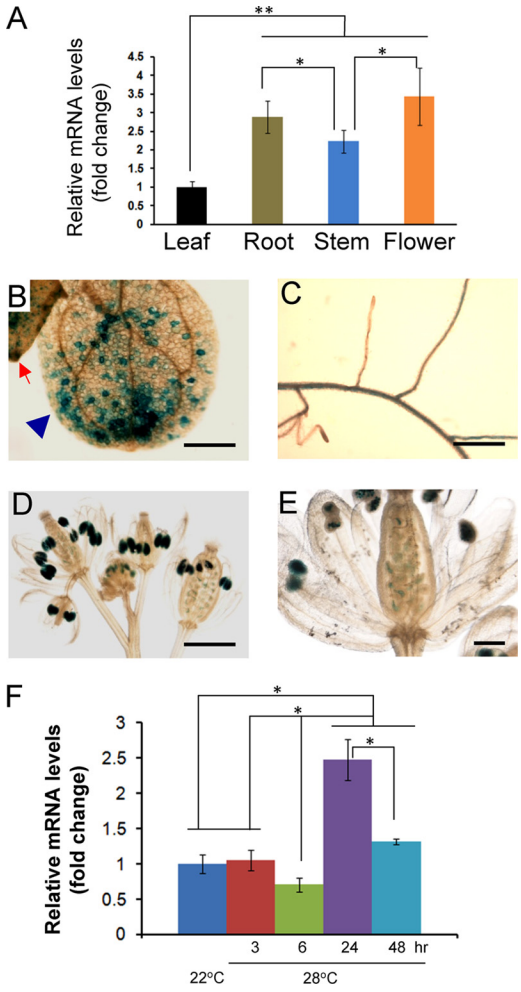

FIGURE 1. **Expression of *AtGRXS17* in *Arabidopsis* and in response to elevated temperature.** *A*, *AtGRXS17* transcripts were detected by quantitative RT-PCR in total RNA extracted from rosette leaves, roots, stems, and flowers of wild type seedlings. Relative mRNA levels were normalized to 18 S rRNA, presented as fold changes, which were analyzed for significance using one-way ANOVA. *, $p < 0.05$; **, $p < 0.001$. *B–E*, *AtGRXS17* promoter GUS expression in cotyledon (*arrowhead*) and young leaf (*arrow*) (*B*), roots (*C*), anthers (*D*), and developing embryos (*E*). *Scale bars*, 50 μm in *B*, 2 mm in *C* and *D*, and 50 μm in *E*. *F*, time course analysis of *AtGRXS17* expression under heat stress. 10-Day-old seedlings were shifted to 28 °C for 3, 6, 24, and 48 h before being harvested for RNA extraction. Control seedlings were kept at 22 °C. Relative mRNA levels were presented as fold changes and analyzed as described in *A*. *, $p < 0.05$.

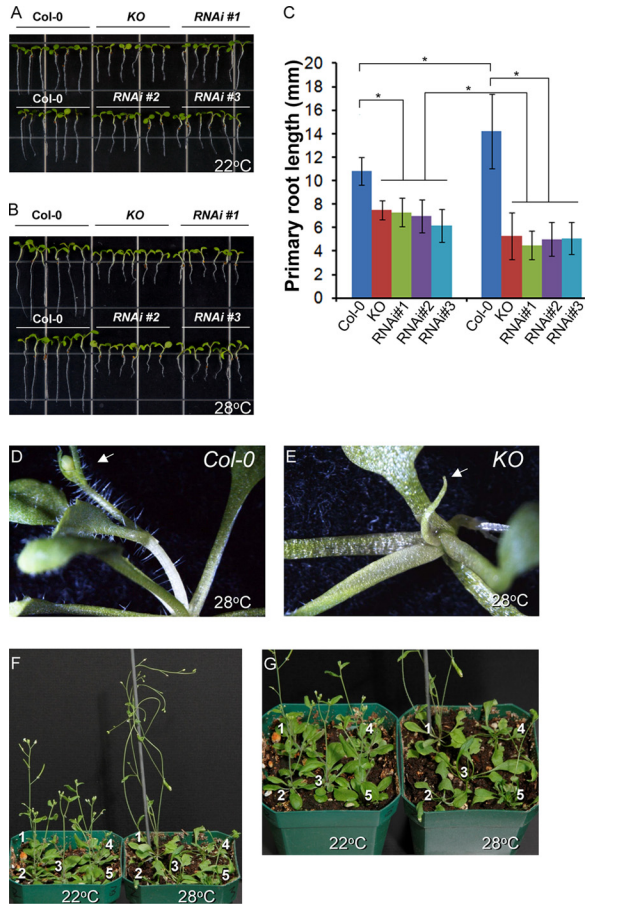

FIGURE 2. ***atgrxs17* KO and RNAi plants were hypersensitive to elevated temperature.** *A–C*, the growth of primary roots in *atgrxs17* KO and RNAi seedlings was slightly reduced at 22 °C (*A* and *C*) and significantly impaired when grown at 28 °C (*B* and *C*). Data were analyzed using two-way ANOVA. *, $p < 0.001$. *D* and *E*, the shoot apices of wild type (*D*) and *atgrxs17* KO (*E*) seedlings grown under 28 °C for 3 weeks showed the pin-like shoot of *atgrxs17* seedlings (*arrow*) under high temperature. *F* and *G*, the growth in *atgrxs17* KO and RNAi plants was inhibited under high temperature. Wild type, *atgrxs17* KO, and three RNAi line seeds were germinated and grown in soil at 22 and 28 °C, respectively, for 6 weeks. Representatives from multiple samples of three independent experiments were shown in *F* and its close-up image in *G*. *1*, wild type controls; *2*, KO plants; *3*, RNAi 1 plants; *4*, RNAi 2 plants; and *5*, RNAi 3 plants.

atgrxs17 KO and AtGRXS17 RNAi Lines Are Hypersensitive to High Temperature—Disruption of *AtGRXS17* led to growth defects at a restrictive temperature (28 °C). The length of primary roots of both KO and RNAi seedlings were reduced ~70% compared with wild type controls, and the growth of both shoots and primary roots was also reduced (Fig. 2, *B* and *C*; supplemental Fig. 1, *D* and *F*). *atgrxs17* KO and RNAi seedling grown at 28 °C showed pin-like shoots in comparison with the normal flower buds on wild type controls (Fig. 2, *D* and *E*). In addition, KO and RNAi plants grown at 28 °C were stunted and arrested in comparison to wild type plants (Fig. 2, *F* and *G*). When grown at 25 °C, *AtGRXS17* loss-of-function plants displayed severe growth defects, such as curled leaves, leafy shoots, and malformed ovule development (supplemental Fig. 2, *A–L*). These results indicate that *AtGRXS17* loss-of-function plants are hypersensitive to temperature changes. In agreement with those observations, biochemical analysis demonstrated that KO and RNAi plants had high ion leakage and accumulated significantly higher amount of anthocyanin compared with wild type controls at 28 °C (supplemental Fig. 3). These data suggest that *AtGRXS17* loss of function leads to significant damage to lipid membranes and changes in stress responses. Notably, the growth inhibition of *atgrxs17* KO and RNAi plants under high temperature was reversible because the same KO plants and RNAi lines reverted to normal growth and seed production when transferred from 28 to 22 °C (supplemental Fig. 2, *M–Q*). These findings indicate that AtGRXS17 is required for postembryonic growth in a temperature-dependent manner.

Auxin Sensitivity of atgrxs17 KO and AtGRXS17 RNAi Lines Is Impaired under High Temperature—The morphological phenotypes of *atgrxs17* KO and RNAi plants at 28 °C (Fig. 2 and supplemental Figs. 1 and 2) were similar to those observed in auxin-related mutants (46). To test whether auxin response is altered in *atgrxs17*, the DR5-GUS reporter line (47) was intro-

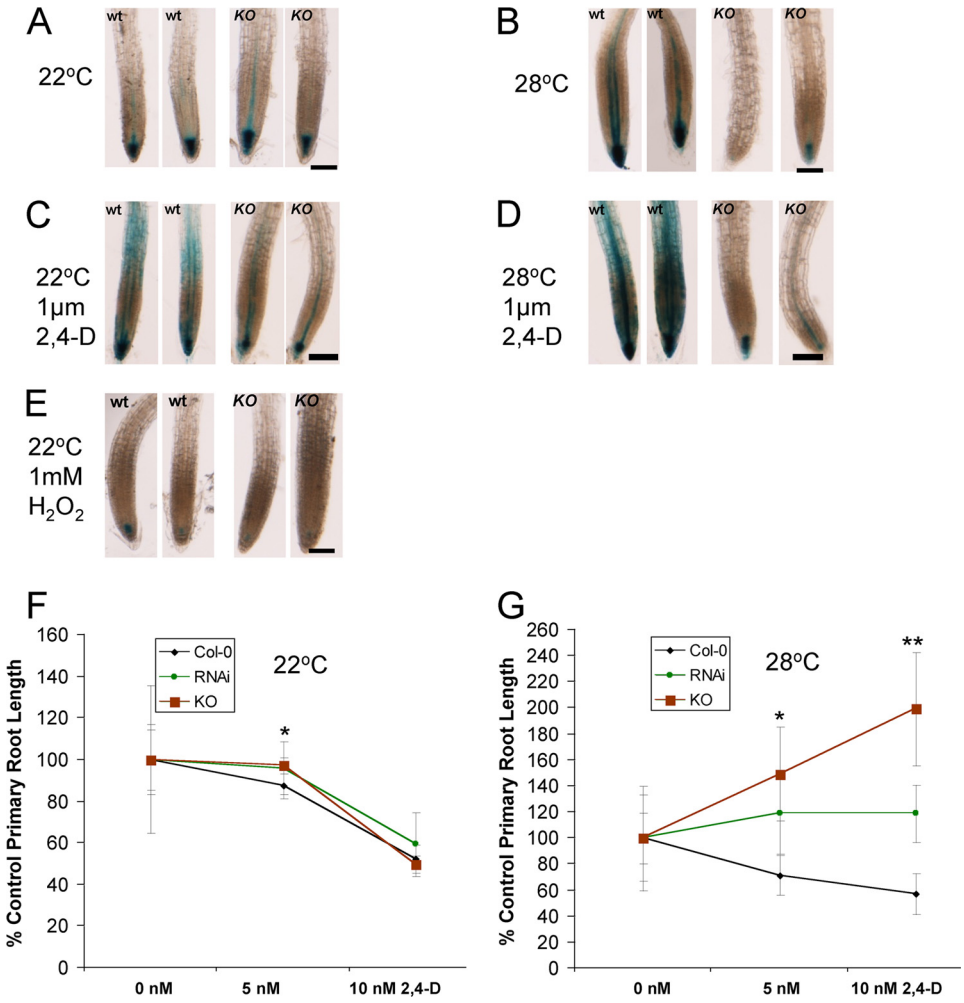

FIGURE 3. **Disruption of *AtGRXS17* altered auxin response under high temperature.** *A–E*, wild type/DR5-GUS and *atgrxs17*/DR5-GUS seeds were germinated and grown on one-half strength MS medium at 22 °C (*A*, *C*, and *E*) and at 28 °C (*B* and *D*) for 7 days. *A*, *C*, and *E*, the seedlings were stained for GUS expression in primary roots at 22 °C without treatment (*A*) or treated with 1 μM 2,4-Dichlorophenoxyacetic acid (*2,4-D*) for 1 h (*C*), or with 1 mM H_2O_2 for 2 h (*E*). Two representative images from each treatment were shown ($n = 30$). No significant difference in GUS expression was seen between wild type controls and KO seedlings within each treatment, but H_2O_2 treatment significantly inhibited GUS expression in both with type and KO seedlings. Two-way ANOVA, $p < 0.001$. *B* and *D*, the seedlings were stained for GUS expression in primary roots at 28 °C without treatment (*B*) or treated with 1 μM 2,4-Dichlorophenoxyacetic acid (*2,4-D*) for 1 h (*D*). GUS expression was significantly reduced in KO seedlings compared with wild type controls. Two-way ANOVA, $p < 0.001$. *Scale bars*, 50 μm. *F* and *G*, *AtGRXS17* loss-of-function seedlings were resistant to exogenous auxin under high temperature. Wild type, *atgrxs17* KO, and RNAi seeds were germinated and grown for 7 days on one-half strength MS medium with or without 2,4-Dichlorophenoxyacetic acid (*2,4-D*) as indicated at 22 °C (*F*) and 28 °C (*G*). The primary root length was measured ($n \geq 30$). Student's *t* test, *, $p < 0.01$; **, $p < 0.0001$.

gressed into the *atgrxs17* KO plants. The DR5-GUS reporter was expressed at a similar level in both *atgrxs17* and wild type controls when grown at 22 °C (Fig. 3*A*). DR5-GUS expression was enhanced at 28 °C in wild type, particularly in the vasculature (Fig. 3*B*). However, DR5-GUS expression was reduced in *atgrxs17* roots under an elevated temperature (Fig. 3*B*), indicating that auxin response was inhibited in *atgrxs17* seedlings. To examine whether the reduced DR5-GUS expression in *atgrxs17* KO plants at 28 °C was due to impaired auxin sensitivity, we tested root growth inhibition by applied auxin. The primary root elongation of wild type seedlings was inhibited by auxin in a dose-dependent manner but independent of temperature treatments (Fig. 3, *F* and *G*), whereas *atgrxs17* KO and RNAi seedlings showed significantly reduced auxin sensitivity at the restrictive temperature (Fig. 3, *F* and *G*). In agreement with this finding, DR5-GUS expression in *atgrxs17* KO plants at 22 °C was reduced in response to exogenous auxin compared with that in control seedlings (Fig. 3*C*). Furthermore, this inhibition of DR5-GUS expression in *atgrxs17* KO plants was more pronounced when the temperature was elevated to 28 °C (Fig. 3*D*). Together, these results demonstrate that the function of AtGRXS17 is required in maintaining auxin sensitivity under high temperature.

Polar Auxin Transport, Not Auxin Levels, Is Altered in atgrxs17 Plants—Auxin-related morphological phenotypes and reduced DR5-GUS expression was observed in *atgrxs17* KO plants (Fig. 3), indicating that they have deficiencies related to auxin action. To test whether IAA levels were altered in *atgrxs17* KO plants, we quantified free and ester-linked IAA in wild type controls and *atgrxs17* KO seedlings grown at 22 and 28 °C. No significant difference in IAA levels was observed between wild type controls and *atgrxs17* KO seedlings at both temperatures (Fig. 4, *A–C*) indicating that the auxin-related phenotypes observed in *atgrxs17* KO plants were not due to altered IAA levels.

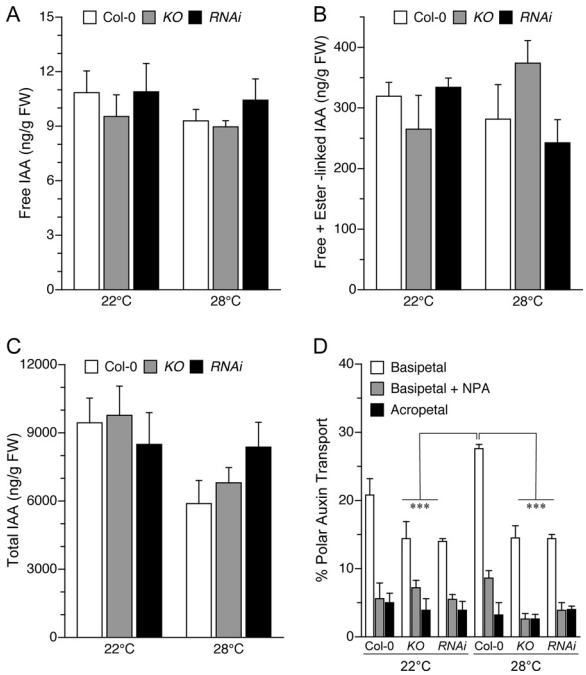

FIGURE 4. **Basipetal polar auxin transport but not auxin content was reduced in *atgrx17* KO and RNAi seedlings grown at elevated temperature.** *A–C*, the levels of free IAA (*A*), free + ester-linked IAA (*B*), and total IAA (*C*) were not significantly changed in *atgrxs17* KO and RNAi seedlings at either 22 or 28 °C. *D*, reduction of polar auxin transport in *atgrxs17* KO and RNAi seedlings at 28 °C. Wild type, *atgrxs17* KO, and RNAi seeds were germinated and grown vertically on one-half strength MS medium at 22 and 28 °C in darkness for 4 days and transferred to continuous cool white fluorescent light (80 μmol m^{-2} s^{-1}) for 2 days. Polar auxin transport was measured. Data are expressed as dpm in the receiver block plus the basal half of the hypocotyl as a % of total dpm in the hypocotyl and the receiver block (*Basipetal*). Controls were run with 10 μM NPA added in the receiver blocks (*Basipetal + NPA*), or an inverted orientation of the hypocotyl section (*Acropetal*). *Error bars* indicate S.E. ($n = 9$) (two-way ANOVA, ***, $p < 0.001$). *FW*, fresh weight.

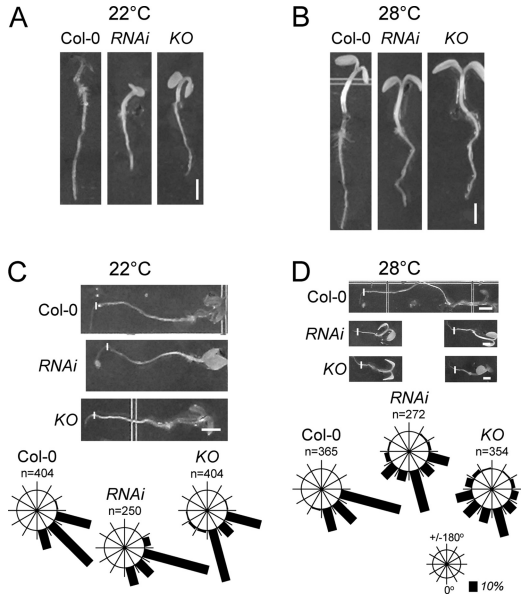

FIGURE 5. ***atgrxs17* KO and RNAi seedlings displayed impaired root gravitropic responses when grown at elevated temperature.** Wild type, *atgrxs17* KO, and *AtGRXS17* RNAi seeds were germinated and grown vertically on one-half stength MS medium at 22 or at 28 °C for 5 days before being gravistimulated for 24 h. *A* and *B*, representatives from wild type controls, *atgrxs17* KO, and *AtGRXS17* RNAi seedlings that were grown at 22 °C (*A*) or at 28 °C (*B*) before gravitropic stimulation. *Scale bars*, 5 mm. *C* and *D*, gravitropic reorientation of wild type controls, *atgrxs17* KO, and *AtGRXS17* RNAi seedling root tips 24 h after the plates were turned 90° clockwise. *White lines* represent root tip positions before reorientation. Quantitative reorientation analyses were conducted. Root angles were determined as the deviation from 0°, representing complete reorientation to the vertical, and grouped in 12 sectors of 30°. *Filled bars* represent relative number of roots as percentage of the total (*n*). Both genotypes (wild type, KO, and RNAi) and temperature treatments significantly affected root gravitropic responses. Data were analyzed using three-way ANOVA, $p < 0.001$.

Reduced root systems (Fig. 2) are characteristic phenotypes for *Arabidopsis* mutants with impaired polar auxin transport (8, 48, 49). We thus performed experiments to determine whether polar auxin transport was altered in *atgrxs17* KO plants. As shown in Fig. 4*D*, basipetal transport of auxin in the elongating hypocotyls of *atgrxs17* KO and RNAi seedlings was reduced compared with wild type controls at 22 °C, but this difference was not statistically significant. At 28 °C, basipetal transport of auxin in the elongating hypocotyls of wild type seedlings increased but not of *atgrxs17* KO and RNAi seedlings. The difference between wild type control seedlings and AtGRXS17 loss-of-function seedlings was significant ($p < 0.001$). However, there was no difference in polar auxin transport activity among *atgrxs17* KO and RNAi seedlings at both temperatures, suggesting that the reduction of basipetal transport of auxin in the elongating hypocotyls of *atgrxs17* KO and RNAi seedlings was independent of temperature treatment. As expected, basipetal auxin transport was greatly reduced by NPA, an inhibitor of polar auxin transport, among wild type controls, *atgrxs17* KO, and RNAi seedlings (Fig. 4*D*). The consistently low acropetal transport indicated a low level of background in the assay (Fig. 4*D*). Interestingly, higher temperatures promoted polar auxin transport in wild type controls, but not in either *atgrxs17* KO or RNAi seedlings (Fig. 4*D*), indicating that temperature-dependent promotion of polar auxin transport was lost in both *atgrxs17* KO and RNAi seedlings. Polar auxin transport has been frequently linked with gravitropism (48). Consistent with the findings of polar auxin transport assays (Fig. 4*D*), impaired gravitropism was observed in both *atgrxs17* KO and RNAi seedlings compared with wild type controls at both temperatures (Fig. 5). Together, these results demonstrate that AtGRXS17 is required for NPA-sensitive polar auxin transport under restrictive temperature and the impaired polar auxin transport at least partly, if not fully, accounts for the temperature-dependent auxin-related defects observed in *AtGXRS17* loss-of-function plants.

Disruption of AtGRXS17 Alters Cell Cycle Progression—Growth defects of *atgrxs17* mutants suggest a unique role of AtGRXS17 in cell proliferation and/or cell cycle control. To clarify the mechanism of AtGRXS17 in this process, a cell cycle reporter (*Cyclin B1;1*-GUS, a G_2 phase marker) was introgressed into the *atgrxs17* KO plants. *Cyclin B1;1*-GUS expression in primary root tips, lateral roots, and shoots was similar in *atgrxs17* KO plants and wild type controls at 22 °C (Fig. 6, *A–F*). At restrictive temperatures, reduced *cyclin B1;1*-GUS activity was noted in *atgrxs17* KO plants, indicating that cell proliferation in the root tips of *atgrxs17* KO plants were inhibited by elevated temperature (Fig. 6, *G–L*). We also observed that the *atgrxs17* KO roots were malformed (Fig. 6, *J–L*), suggesting that the cells may undergo differentiation instead of cell division.

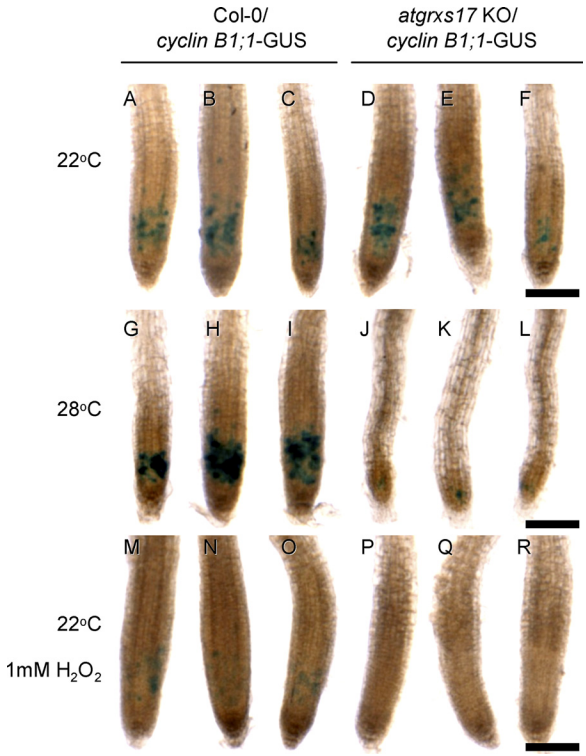

FIGURE 6. **Deficiency in *AtGRXS17* impaired cell cycle progression.** Wild type and *atgrxs17* KO seeds carrying the *cyclinB1;1*-GUS reporter were germinated and grown on one-half strength MS medium at 22 and 28 °C, respectively, for 5 days. One set of seedlings (both wild type/*cyclin B1;1*-GUS and *atgrxs17*/*cyclin B1;1*-GUS seedlings grown at 22 °C) were treated with 1 mM H_2O_2 for 2 h. Histochemical analysis of *cyclin B1;1*-GUS expression was conducted. H_2O_2 treatment significantly inhibited GUS expression in both wild type controls and KO seedlings, whereas GUS expression of KO seedlings grown at 28 °C was significantly reduced compared with wild type controls. Shown are three representative images from each treatment ($n = 30$). Data were analyzed using two-way ANOVA, $p < 0.001$. *Scale bars*, 50 μm.

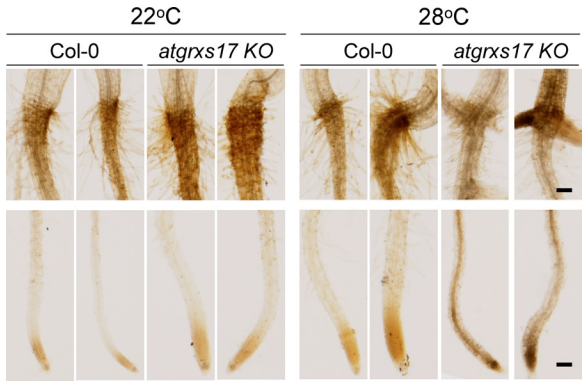

FIGURE 7. **Accumulation of H_2O_2 in wild type and *atgrxs17* KO roots under high temperature.** Wild type and *atgrxs17* KO seeds were germinated and grown on one-half strength MS medium for 10 days at 22 and 28 °C, respectively. Seedlings were stained with diaminobenzidine, and the accumulation of H_2O_2 was indicated by the brown color in primary roots and root-hypocotyl junctions. The root tips and vasculature of KO seedlings significantly accumulated H_2O_2 compared with wild type controls when grown at 28 °C. Shown are two representative images from each treatment ($n = 30$). Data were analyzed using a chi-square test, $p < 0.001$. *Scale bars*, 100 μm.

atgrxs17 KO Seedlings Display Increased ROS Levels—Monothiol Grxs have an antioxidant function in protecting cells against oxidative stress (32, 33, 50). Thus, we hypothesized that AtGRXS17 loss-of-function plants accumulated more ROS than controls. H_2O_2 accumulation was detected by 3,3′-diaminobenzidine staining in wild type and *atgrxs17* KO seedlings. The root tips and the junction areas (between the hypocotyl and the root) displayed more intense staining in AtGRXS17 loss-of-function seedlings than the corresponding area of the wild type seedlings at 28 °C (Fig. 7). Most interestingly, under high temperature, *atgrxs17* KO seedlings accumulated higher amounts of H_2O_2 in vascular bundles (Fig. 7) in comparison with wild type controls. Thus, excess ROS accumulation in particular cell types and tissues could contribute to impaired auxin transport and/or inhibit postembryonic growth at elevated temperatures.

ROS Inhibits Auxin Sensitivity and Compromises Cell Cycle Progression—Given the increased ROS levels in *atgrxs17* KO plants under high temperature (Fig. 7), we hypothesized that excess ROS in *AtGRXS17* loss-of-function roots accounted for the inhibition of auxin response. To test this hypothesis, we treated both wild type controls and *atgrxs17* KO DR5-GUS seedlings with H_2O_2 and then measured DR5-GUS expression. Indeed, exogenous H_2O_2 blocked DR5-GUS expression in wild type seedlings (Fig. 3*E*). The expression of the cell cycle progression marker, *cyclin B1;1*-GUS was also inhibited by H_2O_2 (Fig. 6, *M–R*). Together, these results indicate a critical role of AtGRXS17 in the mechanistic link between ROS and auxin signaling in mediating plant growth and temperature responses.

DISCUSSION

Glutaredoxins have emerged to be key regulators in stress responses and organ development in plants (33, 51, 52). In the present study, we characterized an *Arabidopsis* monothiol glutaredoxin, AtGRXS17, and demonstrated that AtGRXS17 is a critical component involved in ROS accumulation, auxin signaling, and temperature-dependent postembryonic growth in plants.

AtGRXS17 expression is low in comparison with two other *Arabidopsis* monothiol *Grxs*, *AtGRXcp* and *AtGRX4* (Fig. 1, *A–E*) (32, 33). But still, *AtGRXS17* expression appears to be regulated in different tissues and/or organs with lower levels of expression in mature leaves and higher accumulation in flowers (Fig. 1*A*). In contrast to *AtGRXcp* and *AtGRX4*, *AtGRXS17* expression was induced by elevated temperature (Fig. 1*F*), suggesting a unique role in temperature stress responses. Interestingly, time course analysis indicated that *AtGRXS17* expression was induced significantly when seedlings were exposed to higher temperatures for 24 h (Fig. 1*F*). However, we were unable to monitor more rapid responses to elevated temperatures. This finding suggests that *AtGRXS17* may not be involved in the early stages of heat responses in plants but may play a role in protecting plants against the cumulative effects of high temperatures. Alternatively, *AtGRXS17* induction may be due to a secondary effect, such as ROS accumulation caused by heat stress (Fig. 7). Further studies will be required to clarify factors modulating the *AtGRXS17* expression and identification of downstream targets.

Arabidopsis AtGRXS17 deletion mutants do not have any visible defects in seed germination under normal growth conditions (data not shown). However, mutant plants did display

significantly slower growth both as seedlings and as mature flowering plants in comparison to wild type controls under the same growth conditions (Fig. 2; supplemental Figs. 1 and 2). These findings suggest that the presence of *AtGRXS17* in plants is critical for postembryonic growth. Our previous studies report that both AtGRXcp and AtGRX4 are also important for seedling growth (32, 33). Deletion of a single or double CC-type Grx in *Arabidopsis* causes defects in anther development (53). Furthermore, recent genetic analysis of genes that are involved in redox regulation revealed that those genes are also critical in postembryonic growth and organ development (54–57). Together, these studies imply an important mechanism underlying redox regulation in plant development.

The *atgrxs17* mutants are sensitive to restrictive temperature making them distinct from *atgrxcp* and *atgrx4* mutants (Fig. 2; supplemental Figs. 1 and 2). It appears that the sensitivity of *atgrxs17* mutants to high temperature is contingent on both the duration and degree of temperature treatment. For example, at 22 °C, *atgrxs17* mutants displayed slight (but significant) growth defects; at 25 °C, the more severe phenotypes were observed (supplemental Fig. 2, *A–L*); at 28 °C, the growth of *atgrxs17* mutants were drastically inhibited (Fig. 2), which correlated with the high accumulation of ROS detected in the growing tissues (Fig. 7). Furthermore, cell cycle progression in meristematic tissues was blocked in the *atgrxs17* mutants at high temperature (Fig. 6). It is known that excess ROS can cause plant cell cycle arrest and impaired development (58, 59). Our findings support this notion that AtGRXS17 negatively modulates ROS-mediated signaling pathways and protects cells against oxidative stress caused by high temperature.

ROS can act as signals to facilitate hormonal responses involving many physiological processes (3, 22, 23). Recent work has shown H_2O_2 mediates auxin-regulated gravitropic response in roots (20) and high levels of ROS (as found in oxidized environments) closely correlates with the high levels of auxin required for formation and maintenance of stem cell niches in the root quiescent center (60). In this study, the developmental defects observed in *AtGRXS17* loss-of-function plants were shown to be accompanied by increased accumulation of ROS (Figs. 2 and 7), which significantly compromised auxin sensitivity. This was clearly indicated by the reduced DR5-GUS expression (Fig. 3), altered polar auxin transport (Fig. 4), and impaired gravitropic responses (Fig. 5). Thus, our findings suggest that AtGRXS17 may intersect with auxin-mediated signaling to regulate cell growth and development.

The compromised auxin sensitivity in *AtGRXS17* loss-of-function plants was more profound at 28 °C than that at 22 °C (Fig. 3), indicating that auxin-related phenotypes or auxin response in *AtGRXS17* loss-of-function plants was temperature-dependent. Previous studies reported that high temperature can increase the levels of endogenous IAA and promotes hypocotyl elongation (13). The DR5-GUS expression level was induced in wild type roots at 28 °C compared with that at 22 °C (Fig. 3, *A* and *B*), which is consistent with previous reports. Unexpectedly, measurement of endogenous free IAA, conjugated IAA, and total IAA revealed no difference between wild type controls and *AtGRXS17* loss-of-function seedlings under both temperatures (Fig. 4, *A–C*). We speculate this may be due to the different growth conditions (29 °C in the previous study *versus* 28 °C in this study) and/or plant tissues used for IAA measurement (hypocotyls *versus* whole seedlings). This hypocotyl-specific increase in IAA production could be masked by the IAA measurement performed on the whole seedling (61).

Although IAA levels remained unchanged, polar auxin transport activity was increased in wild type controls under high temperature, whereas the induction of polar auxin transport activity was blocked in *AtGRXS17* loss-of-function seedlings under heat stress (Fig. 4*D*). It is conceivable that the reduction of polar auxin transport activity in *AtGRXS17* loss-of-function plants contributes to the auxin-related growth defects under high temperature. Interestingly, the high levels of ROS accumulated along the vascular bundles in *AtGRXS17* loss-of-function seedling roots at a restrictive temperature (Fig. 7). We speculate that this unique oxidizing environment might influence phloem as well as polar transport functions and subsequently inhibit long range auxin as well as carbon transport from the source to the sink tissues (62).

Both ROS and heat stress can disrupt membrane integrity and function (63). Because of the central role of membranes in auxin uptake and transport, the decreased auxin response and polar auxin transport of *AtGRXS17* loss-of-function seedlings under high temperature could be due to indirect effects of membrane dysfunction caused by accumulated ROS or elevated temperature (supplemental Fig. 3*A*). Previous studies indicate that anthocyanins/flavonoids such as quercetin and kaempferol can act as endogenous auxin transport inhibitors (64). It is possible that the increased accumulation of anthocyanin in *AtGRXS17* loss-of-function seedlings at 28 °C (supplemental Fig. 4*B*) might have a role in inhibiting auxin transport in the mutants. Furthermore, auxin responses are mediated by a vast array of auxin-induced or suppressed transcripts (65). There is a possibility that auxin-regulated transcripts at high temperature are dependent on AtGRXS17 function. In support of this notion, *cyclin B1;1*::GUS expression, which is induced by auxin (66, 67), was inhibited in *atgrxs17* KO plants under high temperatures (Fig. 6).

Recent genetic analysis of an *Arabidopsis* triple mutant lacking both Nicotinamide Adenine Dinucleotide Phosphate (NADPH)-dependent thioredoxin reductase (A and B) and glutathione biosynthesis (CAD2) genes revealed that auxin metabolism and polar auxin transport are inhibited when the redox homeostasis was altered in the mutant plants, suggesting crosstalk among redox and auxin signaling systems in controlling plant growth and development (25). Whether AtGRXS17 is involved in this regulatory interplay is still unknown. However, Grxs could be substrates of thioredoxin reductases (68). Our work here establishes a foundation to examine the role of Grxs in redox regulatory mechanisms underlying hormonal responses and adaptation to temperature stresses.

Acknowledgments—We are grateful for Drs. Bonnie Bartel and Elizabeth Vierling for critical reading of the manuscript.

REFERENCES

1. Franklin, K. A. (2009) *Curr. Opin. Plant Biol.* **12,** 63–68
2. Potters, G., Pasternak, T. P., Guisez, Y., and Jansen, M. A. (2009) *Plant Cell*

Environ. **32,** 158–169
3. Beveridge, C. A., Mathesius, U., Rose, R. J., and Gresshoff, P. M. (2007) *Curr. Opin. Plant Biol.* **10,** 44–51
4. Larkindale, J., Hall, J. D., Knight, M. R., and Vierling, E. (2005) *Plant Physiol.* **138,** 882–897
5. Kotak, S., Larkindale, J., Lee, U., von Koskull-Döring, P., Vierling, E., and Scharf, K. D. (2007) *Curr. Opin. Plant Biol.* **10,** 310–316
6. Penfield, S. (2008) *New Phytol.* **179,** 615–628
7. Kumar, S. V., and Wigge, P. A. (2010) *Cell* **140,** 136–147
8. Teale, W. D., Paponov, I. A., and Palme, K. (2006) *Nat. Rev. Mol. Cell Biol.* **7,** 847–859
9. Benjamins, R., and Scheres, B. (2008) *Ann. Rev. Plant Biol.* **59,** 443–465
10. Santner, A., Calderon-Villalobos, L. I., and Estelle, M. (2009) *Nat. Chem. Biol.* **5,** 301–307
11. Vanneste, S., and Friml, J. (2009) *Cell* **136,** 1005–1016
12. Blázquez, M. A., Ahn, J. H., and Weigel, D. (2003) *Nat. Genet.* **33,** 168–171
13. Gray, W. M., Ostin, A., Sandberg, G., Romano, C. P., and Estelle, M. (1998) *Proc. Natl. Acad. Sci. U.S.A.* **95,** 7197–7202
14. Ludwig-Müller, J., Krishna, P., and Forreiter, C. (2000) *Plant Physiol.* **123,** 949–958
15. Toh, S., Imamura, A., Watanabe, A., Nakabayashi, K., Okamoto, M., Jikumaru, Y., Hanada, A., Aso, Y., Ishiyama, K., Tamura, N., Iuchi, S., Kobayashi, M., Yamaguchi, S., Kamiya, Y., Nambara, E., and Kawakami, N. (2008) *Plant Physiol.* **146,** 1368–1385
16. Foyer, C. H., and Noctor, G. (2009) *Antiox. Redox Signal.* **11,** 861–905
17. Sagi, M., and Fluhr, R. (2006) *Plant Physiol.* **141,** 336–340
18. Pitzschke, A., Forzani, C., and Hirt, H. (2006) *Antioxid. Redox Signal.* **8,** 1757–1764
19. Miller, G., Shulaev, V., and Mittler, R. (2008) *Physiol. Plant* **133,** 481–489
20. Joo, J. H., Bae, Y. S., and Lee, J. S. (2001) *Plant Physiol.* **126,** 1055–1060
21. Foreman, J., Demidchik, V., Bothwell, J. H., Mylona, P., Miedema, H., Torres, M. A., Linstead, P., Costa, S., Brownlee, C., Jones, J. D., Davies, J. M., and Dolan, L. (2003) *Nature* **422,** 442–446
22. Kwak, J. M., Nguyen, V., and Schroeder, J. I. (2006) *Plant Physiol.* **141,** 323–329
23. Gapper, C., and Dolan, L. (2006) *Plant Physiol.* **141,** 341–345
24. Achard, P., Renou, J. P., Berthomé, R., Harberd, N. P., and Genschik, P. (2008) *Current Biology* **18,** 656–660
25. Bashandy, T., Guilleminot, J., Vernoux, T., Caparros-Ruiz, D., Ljung, K., Meyer, Y., and Reichheld, J. P. (2010) *Plant Cell* **22,** 376–391
26. Meyer, Y., Buchanan, B. B., Vignols, F., and Reichheld, J. P. (2009) *Annu Rev Genet* **43,** 335–367
27. Lillig, C. H., Berndt, C., and Holmgren, A. (2008) *Biochim Biophys Acta* **1780,** 1304–1317
28. Lemaire, S. D. (2004) *Photosynth Res* **79,** 305–318
29. Rouhier, N., Couturier, J., and Jacquot, J. P. (2006) *J Exp Bot* **57,** 1685–1696
30. Rouhier, N., Gelhaye, E., and Jacquot, J. P. (2004) *Cell. Mol. Life Sci.* **61,** 1266–1277
31. Ndamukong, I., Abdallat, A. A., Thurow, C., Fode, B., Zander, M., Weigel, R., and Gatz, C. (2007) *Plant J.* **50,** 128–139
32. Cheng, N. H., Liu, J. Z., Brock, A., Nelson, R. S., and Hirschi, K. D. (2006) *J. Biol. Chem.* **281,** 26280–26288
33. Cheng, N. H. (2008) *FEBS Lett.* **582,** 848–854
34. Alonso, J. M., Stepanova, A. N., Leisse, T. J., Kim, C. J., Chen, H., Shinn, P., Stevenson, D. K., Zimmerman, J., Barajas, P., Cheuk, R., Gadrinab, C., Heller, C., Jeske, A., Koesema, E., Meyers, C. C., Parker, H., Prednis, L., Ansari, Y., Choy, N., Deen, H., Geralt, M., Hazari, N., Hom, E., Karnes, M., Mulholland, C., Ndubaku, R., Schmidt, I., Guzman, P., Aguilar-Henonin, L., Schmid, M., Weigel, D., Carter, D. E., Marchand, T., Risseeuw, E., Brogden, D., Zeko, A., Crosby, W. L., Berry, C. C., and Ecker, J. R. (2003) *Science* **301,** 653–657
35. Liu, C. J., Blount, J. W., Steele, C. L., and Dixon, R. A. (2002) *Proc. Natl. Acad. Sci. U.S.A.* **99,** 14578–14583
36. Clough, S. J., and Bent, A. F. (1998) *Plant J.* **16,** 735–743
37. Mei, H., Cheng, N. H., Zhao, J., Park, S., Escareno, R. A., Pittman, J. K., and Hirschi, K. D. (2009) *New Phytol.* **183,** 95–105
38. Czechowski, T., Stitt, M., Altmann, T., Udvardi, M. K., and Scheible, W. R. (2005) *Plant Physiol.* **139,** 5–17
39. Men, S., Boutté, Y., Ikeda, Y., Li, X., Palme, K., Stierhof, Y. D., Hartmann, M. A., Moritz, T., and Grebe, M. (2008) *Nat. Cell Biol.* **10,** 237–244
40. Gallois, J. L., Woodward, C., Reddy, G. V., and Sablowski, R. (2002) *Development* **129,** 3207–3217
41. Hodges, D. M., DeLong, J. M., Forney, C. F., and Prange, R. K. (1999) *Planta* **207,** 604–611
42. Ilić, N., Normanly, J., and Cohen, J. D. (1996) *Plant Physiol.* **111,** 781–788
43. Barkawi, L. S., Tam, Y. Y., Tillman, J. A., Normanly, J., and Cohen, J. D. (2010) *Nat. Protoc.* **5,** 1609–1618
44. Gardner, G., and Sanborn, J. R. (1989) *Plant Physiol.* **90,** 291–295
45. Lewis, D. R., and Muday, G. K. (2009) *Nat. Protoc.* **4,** 437–451
46. Gälweiler, L., Guan, C., Müller, A., Wisman, E., Mendgen, K., Yephremov, A., and Palme, K. (1998) *Science* **282,** 2226–2230
47. Ulmasov, T., Murfett, J., Hagen, G., and Guilfoyle, T. J. (1997) *Plant Cell* **9,** 1963–1971
48. Muday, G. K., and DeLong, A. (2001) *Trends Plant Sci.* **6,** 535–542
49. Tanaka, H., Dhonukshe, P., Brewer, P. B., and Friml, J. (2006) *Cell Mol. Life Sci.* **63,** 2738–2754
50. Herrero, E., and de la Torre-Ruiz, M. A. (2007) *Cell Mol. Life Sci.* **64,** 1518–1530
51. Li, S., Lauri, A., Ziemann, M., Busch, A., Bhave, M., and Zachgo, S. (2009) *Plant Cell* **21,** 429–441
52. Sundaram, S., and Rathinasabapathi, B. (2010) *Planta* **231,** 361–369
53. Xing, S., and Zachgo, S. (2008) *Plant J.* **53,** 790–801
54. Vernoux, T., Wilson, R. C., Seeley, K. A., Reichheld, J. P., Muroy, S., Brown, S., Maughan, S. C., Cobbett, C. S., Van Montagu, M., Inzé, D., May, M. J., and Sung, Z. R. (2000) *Plant Cell* **12,** 97–110
55. Reichheld, J. P., Khafif, M., Riondet, C., Droux, M., Bonnard, G., and Meyer, Y. (2007) *Plant Cell* **19,** 1851–1865
56. Benitez-Alfonso, Y., Cilia, M., San Roman, A., Thomas, C., Maule, A., Hearn, S., and Jackson, D. (2009) *Proc. Natl. Acad. Sci. U.S.A.* **106,** 3615–3620
57. Marty, L., Siala, W., Schwarzländer, M., Fricker, M. D., Wirtz, M., Sweetlove, L. J., Meyer, Y., Meyer, A. J., Reichheld, J. P., and Hell, R. (2009) *Proc. Natl. Acad. Sci. U.S.A.* **106,** 9109–9114
58. Reichheld, J. P., Vernoux, T., Lardon, F., Van Montagu, M., and Inzé, D. (1999) *Plant J.* **17,** 647–656
59. Vranová, E., Atichartpongkul, S., Villarroel, R., Van Montagu, M., Inzé, D., and Van Camp, W. (2002) *Proc. Natl. Acad. Sci. U.S.A.* **99,** 10870–10875
60. Jiang, K., Meng, Y. L., and Feldman, L. J. (2003) *Development* **130,** 1429–1438
61. Zhao, Y., Hull, A. K., Gupta, N. R., Goss, K. A., Alonso, J., Ecker, J. R., Normanly, J., Chory, J., and Celenza, J. L. (2002) *Genes Dev.* **16,** 3100–3112
62. Robert, H. S., and Friml, J. (2009) *Nat. Chem. Biol.* **5,** 325–332
63. Vigh, L., Nakamoto, H., Landry, J., Gomez-Munoz, A., Harwood, J. L., and Horvath, I. (2007) *Ann. N.Y. Acad. Sci.* **1113,** 40–51
64. Taylor, L. P., and Grotewold, E. (2005) *Curr. Opin. Plant Biol.* **8,** 317–323
65. Chapman, E. J., and Estelle, M. (2009) *Ann. Rev. Genet.* **43,** 265–285
66. De Veylder, L., Beeckman, T., and Inzé, D. (2007) *Nat. Rev. Mol. Cell Biol.* **8,** 655–665
67. Vanneste, S., De Rybel, B., Beemster, G. T., Ljung, K., De Smet, I., Van Isterdael, G., Naudts, M., Iida, R., Gruissem, W., Tasaka, M., Inzé, D., Fukaki, H., and Beeckman, T. (2005) *Plant Cell* **17,** 3035–3050
68. Zaffagnini, M., Michelet, L., Massot, V., Trost, P., and Lemaire, S. D. (2008) *J. Biol. Chem.* **283,** 8868–8876

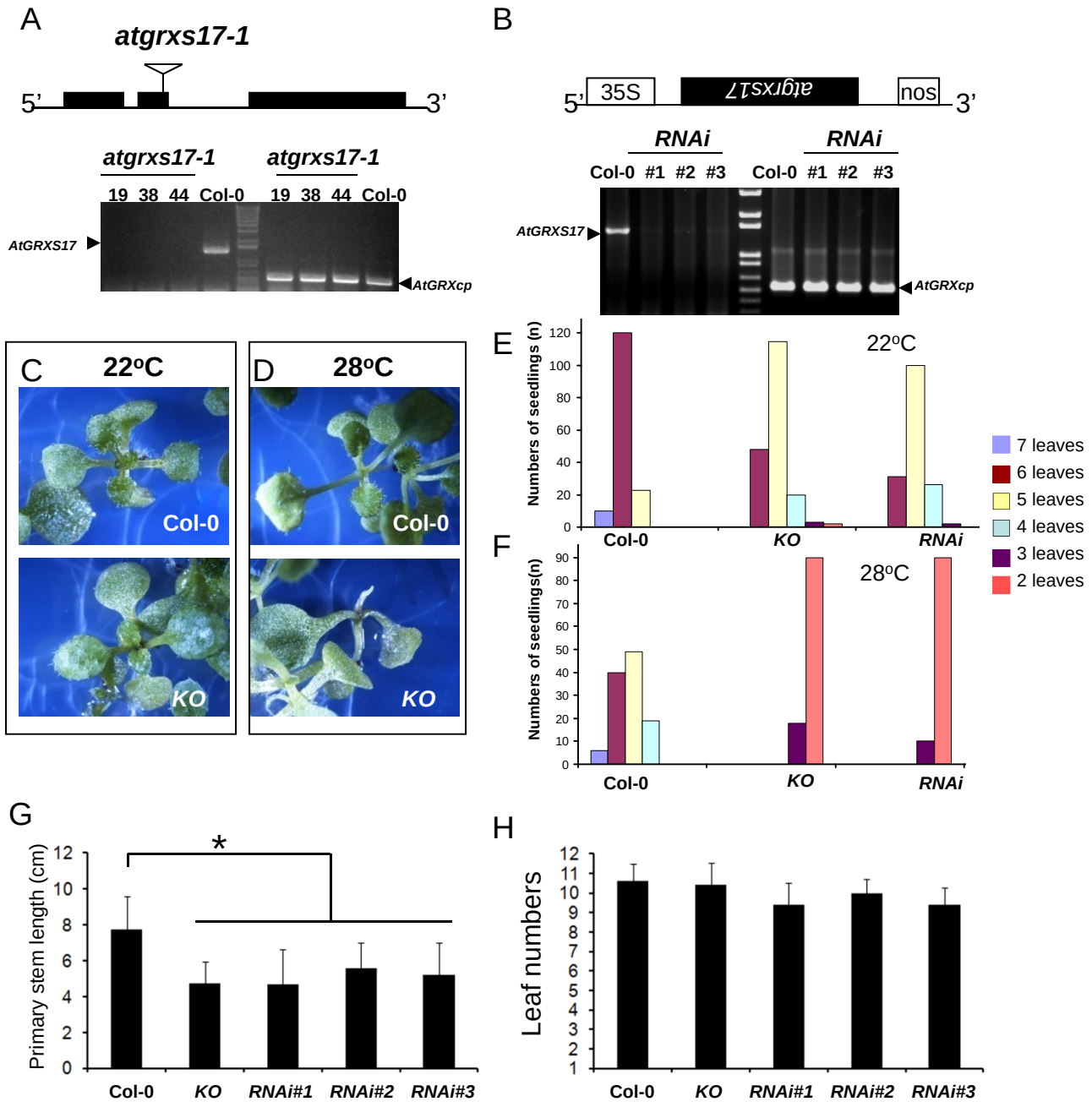

Suppl.Fig.1. *AtGRXS17* loss-of-function plants are defective in vegetative growth and sensitive to high temperature. *A*. The top panel describes the *AtGRXS17* genomic DNA structure and locations of a T-DNA insertion line. Filled boxes indicate exons and line indicates introns. AtGRXS17 RNA transcripts were not detectable in three *atgrxs17-1* plants. *B.* The top panel shows the RNAi (antisense) construct. *AtGRXS17* RNA transcripts were detected by semi-quantitative RT-PCR and results indicate *AtGRXS17* expression was reduced in three RNAi lines. *C* and *D. atgrxs17* KO seedlings showed growth defects in shoots at 22°C (*C*) and 28°C (*D*). Elevated temperature (28°C) completely inhibited the growth of new leaves in *AtGRXS17* loss-of-function seedlings. *E* and *F*. The numbers of leaves were counted for 10-day-old wild type controls and *AtGRXS17* loss-of-function seedlings grown at 22°C (*E*) and 28°C (*F*). At 22°C, most of wild type seedlings have 6 or more leaves, while the majority of *AtGRXS17* loss-of-function seedlings have 5 leaves or less (*E*), and when grown at 28°C, almost no new leaves were grown in *AtGRXS17* loss-of-function seedlings (*F*). *G*. *atgrxs17* KO and RNAi plant phenotypes. Wild type, *atgrxs17* KO, and RNAi line seeds were germinated and grown in soil under normal growth condition (greenhouse) for 6 weeks. The results indicated that *atgrxs17* KO and RNAi#1 plants grew significantly slow in comparison to wild type controls. One-way ANOVA, *p<0.05. *H*. Effect of *AtGRXS17* expression on flowering time. The numbers of leaves of wild type, *atgrxs17* KO, and RNAi plants grown under normal conditions for six weeks were counted. The results indicated that there was no difference in flowering time among wild type, KO, and RNAi plants even though KO and RNAi plants grew slowly compared to wild type plants. One-way ANOVA, p=0.961.

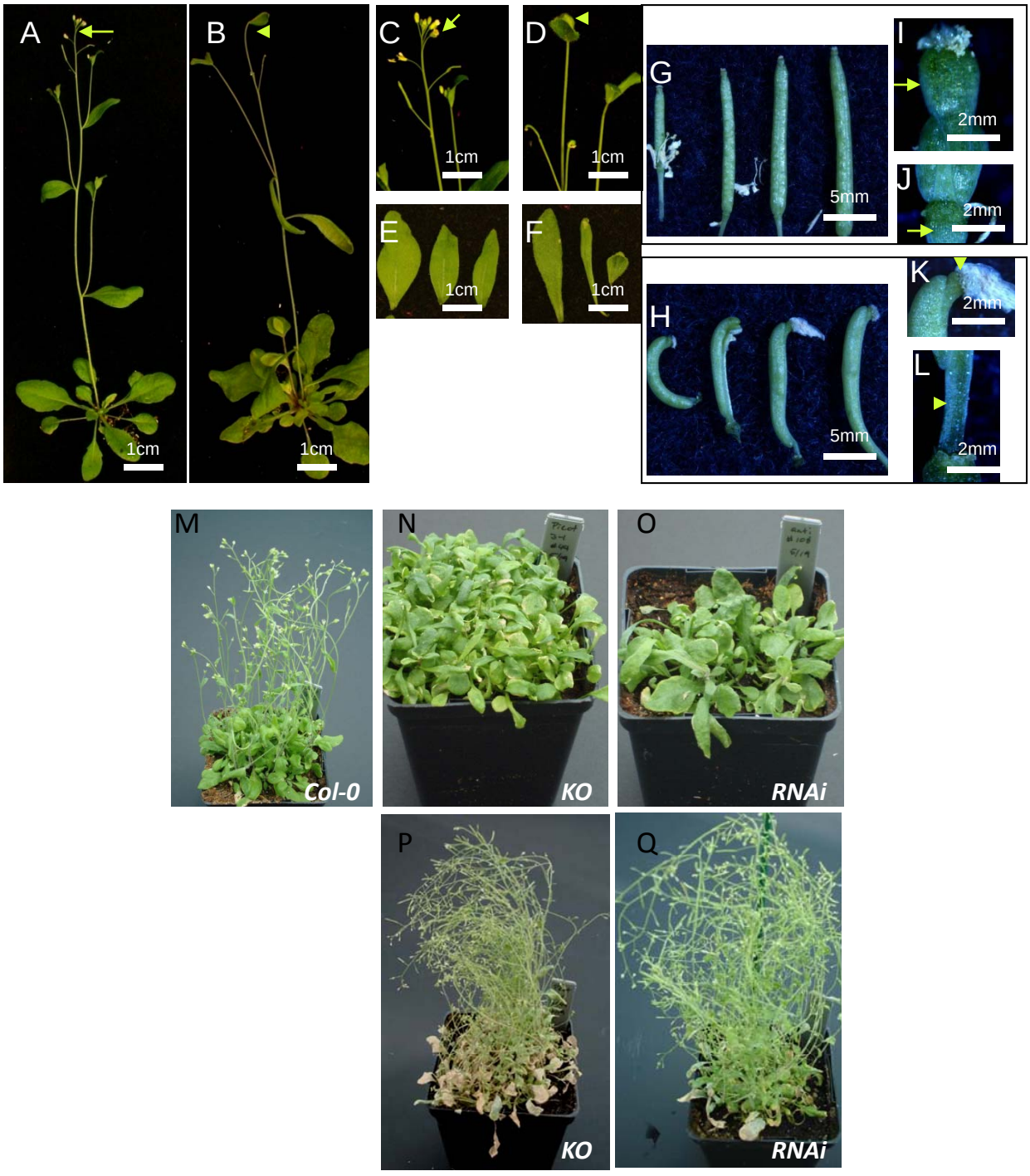

Suppl.Fig.2. Effect of *AtGRXS17* expression on plant growth is temperature-dependent. *A-L*. *atgrxs17* KO plants displayed defects grown at 25°C. *atgrxs17* KO plants grew slowly with long narrow petioles and irregular shaped leaves, leafy shoot apices (arrowhead), and lateral branches (*B*, *D*, and *F*) in comparison to wild type plants (*A, C, E*). The development of gyneocium in *atgrxs17* KO plants (*H*) was also impaired compared to wild type (*G*) with only one valve, abnormal stigmas (*K*), and extended internodes (*L*) indicated by arrowheads compared to wild type normal stigmas (*I*) and internodes (*J*) indicated by arrows. *M-Q*. High temperature-inhibition of growth in *atgrxs17* KO and RNAi plants was reversible. Wild type, *atgrxs17* KO, and RNAi seeds were germinated and grown in soil under high temperature (28°C for 16 hr during daytime and 25°C for 8 hr at night) for 7 weeks (*M-O*). After transferred to normal growth condition (22°C) for an additional 7 weeks, the same *atgrxs17* KO and RNAi plants regained normal growth and produced seeds (*P and Q*).

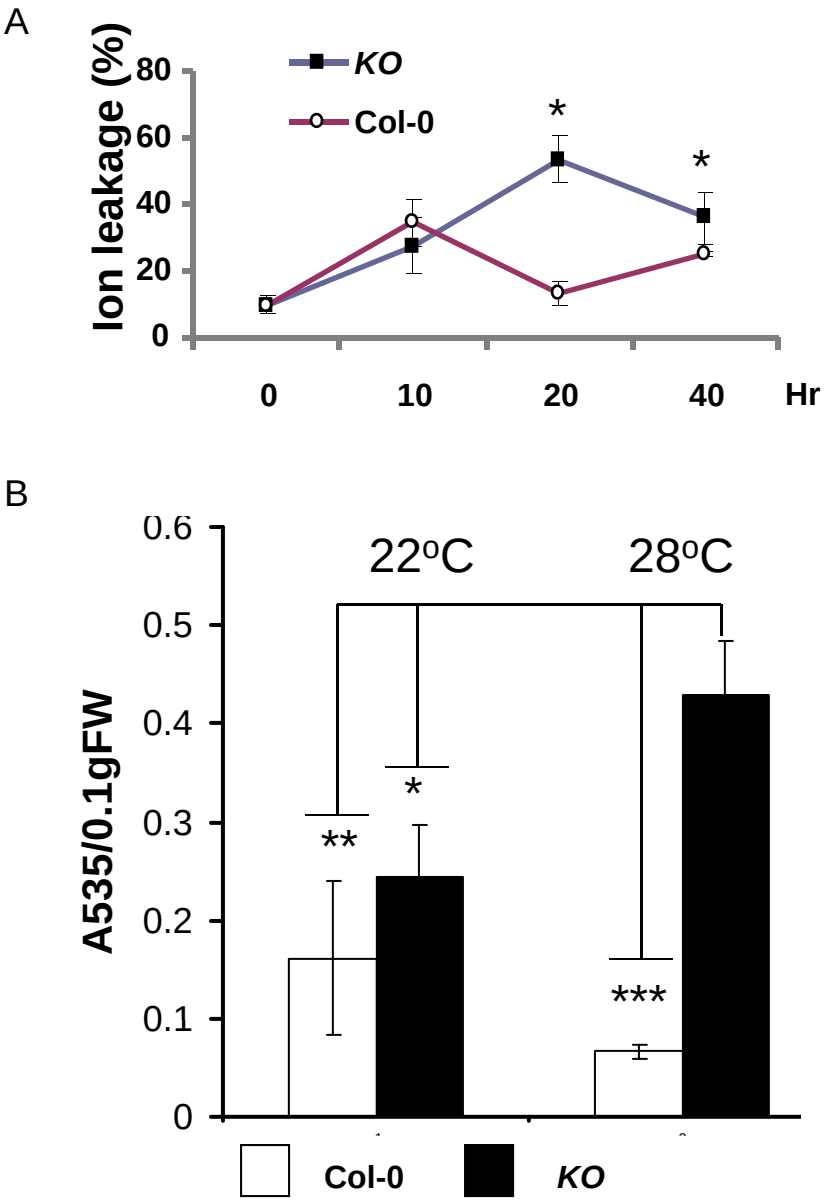

Suppl.Fig.3. Biochemical analysis of *atgrxs17* KO plants under high temperature. *A.* Arabidopsis heat tolerant test with wild-type (Col-0) and *atgrxs17* plants. Four-week-old Arabidopsis plants were exposed to temperature 38ºC for 10 hrs, 20 hrs and 40 hrs, respectively. Percent leakage of ions of Arabidopsis in response to heat stress was measured. The error bar represents standard deviation (n=5). The asterisk (*****) is statistical difference by Student *t* test ($p<0.05$). *B.* Anthocyanin quantitation of Arabidopsis wild type and *atgrxs17* KO plants. Wild type and *atgrxs17* KO seeds were germinated and grown on ½MS media for two weeks at 22ºC and 28ºC, respectively. Whole seedlings were collected for measuring anthocyanin contents. Student *t* test * $p<0.05$; ** $p<0.01$; *** $p<0.001$.

Plant Biology:

Arabidopsis Monothiol Glutaredoxin, AtGRXS17, Is Critical for Temperature-dependent Postembryonic Growth and Development via Modulating Auxin Response

Ning-Hui Cheng, Jian-Zhong Liu, Xing Liu, Qingyu Wu, Sean M. Thompson, Julie Lin, Joyce Chang, Steven A. Whitham, Sunghun Park, Jerry D. Cohen and Kendal D. Hirschi

J. Biol. Chem. 2011, 286:20398-20406.
doi: 10.1074/jbc.M110.201707 originally published online April 22, 2011